

## OPEN

# $\beta$ 7-Integrin exacerbates experimental DSS-induced colitis in mice by directing inflammatory monocytes into the colon

A Schippers<sup>1,3</sup>, M Muschaweck<sup>1,3</sup>, T Clahsen<sup>1</sup>, S Tautorat<sup>1</sup>, L Grieb<sup>1</sup>, K Tenbrock<sup>1</sup>, N Gaßler<sup>2</sup> and N Wagner<sup>1</sup>

Leukocyte recruitment is pivotal for the initiation and perpetuation of inflammatory bowel disease (IBD) and controlled by the specificity and interactions of chemokines and adhesion molecules. Interactions of the adhesion molecules  $\alpha$ 4 $\beta$ 7-integrin and mucosal addressin cell-adhesion molecule-1 (MAdCAM-1) promote the accumulation of pathogenic T-cell populations in the inflamed intestine. We aimed to elucidate the significance of  $\beta$ 7-integrin expression on innate immune cells for the pathogenesis of IBD. We demonstrate that  $\beta$ 7-integrin deficiency protects recombination-activating gene-2 (RAG-2)-deficient mice from dextran sodium sulfate (DSS)-induced colitis and coincides with decreased numbers of colonic effector monocytes. We also show that  $\beta$ 7-integrin is expressed on most CD11b<sup>+</sup> CD64<sup>low</sup> Ly6C<sup>+</sup> bone marrow progenitors and contributes to colonic recruitment of these proinflammatory monocytes. Importantly, adoptive transfer of CD115<sup>+</sup> wild-type (WT) monocytes partially restored the susceptibility of RAG-2/ $\beta$ 7-integrin double-deficient mice to DSS-induced colitis, thereby demonstrating the functional importance of  $\beta$ 7-integrin-expressing monocytes for the development of DSS colitis. We also reveal that genetic ablation of MAdCAM-1 ameliorates experimental colitis in RAG-2-deficient mice as well. In summary, we demonstrate a previously unknown role of  $\alpha$ 4 $\beta$ 7-integrin–MAdCAM-1 interactions as drivers of colitis by directing inflammatory monocytes into the colon.

## INTRODUCTION

The recirculation of leukocytes is regulated by migration pathways that are secured by the specificity and interactions of chemokines and adhesion molecules.<sup>1</sup> Regulated expression and activation of these molecules helps to initiate and terminate physiologic inflammatory processes. Inappropriate expression, however, can cause a massive and destructive infiltration of leukocytes, leading to tissue inflammation and chronic manifestations. An abnormal cell influx into the inflamed intestine is a prominent histopathologic feature and is fundamental to the development and perpetuation of inflammatory bowel disease (IBD).<sup>2</sup> Hence, there is a great need to better understand leukocyte trafficking, which is a major target for IBD therapy.

The lymphocyte adhesion molecule  $\beta$ 7-integrin directs the migration of lymphocytes into the gut-associated lymphoid

tissue.<sup>3,4</sup> Integrins are heterodimeric transmembrane cell adhesion receptors consisting of noncovalently associated  $\alpha$  and  $\beta$  chains. The  $\beta$ 7-integrin chain combines with either the  $\alpha$ 4 or the  $\alpha$ E (CD103) chain. Whereas  $\alpha$ E $\beta$ 7-integrin facilitates the retention of lymphocytes in the gut epithelium through binding to E-cadherin,  $\alpha$ 4 $\beta$ 7-integrin directs the migration of lymphocytes into the small intestine and into the mesenteric lymph nodes mainly via interaction with its endothelial ligand mucosal addressin cell-adhesion molecule-1 (MAdCAM-1). MAdCAM-1 is a cell-surface, immunoglobulin-like adhesion molecule that belongs to the immunoglobulin superfamily.<sup>5</sup> It is predominantly expressed on high endothelial venules of the gut-associated lymphoid tissue and on venules at chronically inflamed sites.<sup>6</sup> Similar to  $\alpha$ 4 $\beta$ 7-integrin, L-selectin is able to adhere to MAdCAM-1,<sup>7</sup> and also to carbohydrate moieties

<sup>1</sup>Department of Pediatrics, Medical Faculty, RWTH Aachen University, Aachen, Germany and <sup>2</sup>Institute of Pathology, Klinikum Braunschweig, Braunschweig, Germany. Correspondence: N Wagner (nwagner@ukaachen.de)

<sup>3</sup>Authors share cofirst authorship.

Received 9 January 2015; accepted 6 August 2015; published online 9 September 2015. doi:10.1038/mi.2015.82

presented on glycoprotein scaffolds.<sup>8</sup> A further ligand for  $\alpha 4\beta 7$ -integrin is the vascular cell adhesion molecule-1, although this interaction is reported to require a higher state of integrin activation in comparison with MAdCAM-1 binding.<sup>9</sup> This diversity of receptor–ligand interactions, which is made even more complicated by redundant mechanisms of leukocyte trafficking, makes unraveling of the physiologic roles of the individual adhesion molecules particularly difficult.

A role for  $\alpha 4\beta 7$ –MAdCAM-1 interactions in directing lymphocytes to the intestine is widely accepted and inflammation of the intestine is associated with an enhanced expression of MAdCAM-1 and an increased density of  $\alpha 4\beta 7$ -integrin-positive cells in the colonic lamina propria of both experimental animals and humans.<sup>4,6,10</sup> Moreover, vedolizumab, a humanized monoclonal antibody that specifically targets the  $\alpha 4\beta 7$  heterodimer, is effective in treating IBD.<sup>11</sup> Previously, we have shown that the onset of colitis was delayed significantly in recipients of T cells from  $\beta 7$ -integrin-deficient ( $\beta 7$ -integrin  $\Delta/\Delta$  or  $\beta 7 \Delta/\Delta$ ) donors in the CD4<sup>+</sup>CD45RB<sup>high</sup> model of T-cell transfer colitis,<sup>12</sup> which indicates the importance of  $\beta 7$ -integrin on effector T cells in the induction and perpetuation of IBD. To extend this study, we chose to analyze the role of  $\beta 7$ -integrin for innate immune cells in a model where lymphocytes are not essential for colonic inflammation. Oral administration of dextran sodium sulfate (DSS) in the drinking water of mice is a widely used IBD model.<sup>13,14</sup> It causes an acute and chronic colitis in mice with some morphological changes similar to human ulcerative colitis, including an increased expression of adhesion molecules, infiltration of leukocytes, production of inflammatory mediators, and gut injury.<sup>14</sup> It is a relevant model for the translation of data from mice to humans, as it has been shown to respond to drugs used in IBD therapy.<sup>15</sup> DSS acts mainly by breaching the intestinal barrier function, thereby exposing subepithelial immune cells to commensal bacteria and is relatively independent of lymphocyte actions, as mice lacking T cells, B cells, and NK cells can still develop colitis in response to DSS.<sup>16,17</sup>

By a comparative analysis of  $\beta 7$ -integrin  $\Delta/\Delta$  mice, wild-type (WT) mice, RAG-2/ $\beta 7$ -integrin double-deficient mice, RAG-2-deficient (RAG-2  $\Delta/\Delta$ ) mice, and RAG-2/MAdCAM-1 double-deficient mice in the DSS model, we have been able to point out the importance of  $\alpha 4\beta 7$ –MAdCAM-1 interactions for innate immune cells in the induction and perpetuation of IBD.

## RESULTS

### $\beta 7$ -Integrin promotes acute and chronic DSS-induced colitis

To assess the impact of  $\beta 7$ -integrin on the development of acute colitis, WT and  $\beta 7$  integrin  $\Delta/\Delta$  mice were exposed to 3% DSS in the drinking water. DSS treatment induced a substantial weight loss in WT mice, which was less pronounced in  $\beta 7$ -integrin  $\Delta/\Delta$  mice (**Figure 1a**). In addition, compared with  $\beta 7$ -integrin  $\Delta/\Delta$  mice, WT mice exhibited an elevated cumulative disease activity index (DAI) (**Figure 1b**). All vehicle control (i.e. regular water) mice were negative for weight

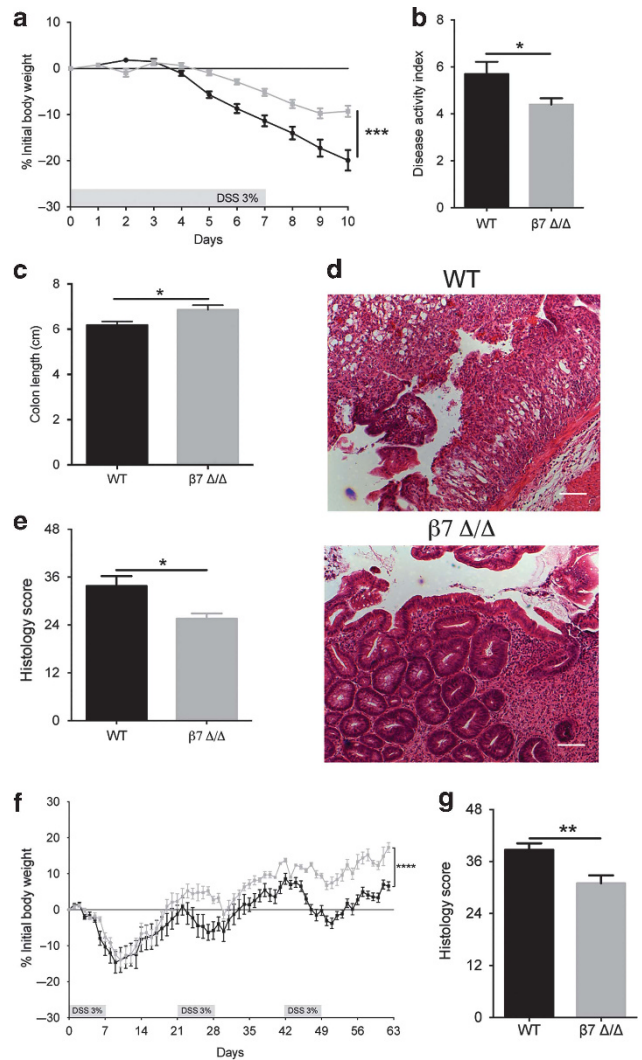


**Figure 1**  $\beta 7$ -Integrin deficiency ameliorates acute (**a–e**) and chronic (**f** and **g**) dextran sodium sulfate (DSS)-induced colitis. (**a**) Percentage of body weight loss (measured daily) of wild-type (WT) (black squares,  $n=12$ ) and  $\beta 7$ -integrin-deficient ( $\beta 7 \Delta/\Delta$ ) (gray squares,  $n=12$ ) mice. (**b**) Disease activity index (DAI) and (**c**) colon length from DSS-treated WT (black bar,  $n=12$ ) and  $\beta 7 \Delta/\Delta$  (gray bar,  $n=12$ ) mice at day 10 of acute DSS colitis. (**d**) Representative photomicrographs of hematoxylin and eosin (H&E)-stained colon sections from the indicated groups at day 10 of acute DSS colitis at original magnification  $\times 100$  (Bar = 200  $\mu\text{m}$ ). (**e**) Results of histological scoring of sections from WT (black bar,  $n=4$ ) and  $\beta 7 \Delta/\Delta$  (gray bar,  $n=5$ ) mice. The data shown are representative of three independent experiments. (**f**) Percentage of body weight loss (measured daily) of WT (black squares,  $n=7$ ) and  $\beta 7 \Delta/\Delta$  (gray squares,  $n=6$ ) mice. (**g**) Results of histological scoring of sections from WT (black bar,  $n=7$ ) and  $\beta 7 \Delta/\Delta$  (gray bar,  $n=6$ ) mice. The data shown are representative of two independent experiments. Data represent mean  $\pm$  s.e.m. Statistical significance was calculated by two-tailed  $t$ -test and is indicated as follows: \* $P < 0.05$ ; \*\* $P < 0.01$ ; \*\*\* $P < 0.001$ , \*\*\*\* $P < 0.0001$ .

loss and are therefore not graphed. Moreover, the reduction in colon length, which is a marker of intestinal inflammation, was significantly less pronounced in DSS-treated  $\beta 7$ -integrin  $\Delta/\Delta$  mice, when compared with equally treated WT mice (**Figure 1c**). As expected, DSS treatment induced a severe inflammatory response in WT mice, with an almost complete

loss of crypts, dense infiltrates of leukocytes in both mucosa and submucosa, and thickening of the bowel wall. By contrast, the infiltrates in DSS-treated  $\beta 7$ -integrin  $\Delta/\Delta$  mice were much smaller and less tissue damage was observed (Figure 1d). Histological scoring for inflammatory infiltrates and epithelial damage confirmed these findings as significant (Figure 1e). We also studied the impact of  $\beta 7$ -integrin on the development of chronic DSS colitis by subjecting  $\beta 7$ -integrin  $\Delta/\Delta$  mice and WT mice to three 7-day cycles of DSS administration, each followed by 14 days of regular drinking water. DSS-treated  $\beta 7$ -integrin  $\Delta/\Delta$  mice exhibited a reduced loss in body weight (Figure 1f), and an improved stool consistency and diminished fecal occult blood, when compared with DSS-treated WT mice. The clinically observed attenuation of chronic intestinal inflammation in  $\beta 7$ -integrin  $\Delta/\Delta$  mice was corroborated by histopathologic evaluation that featured reduced numbers of mucosal erosions, smaller ulcerations, lower hyperplasia, and decreased inflammatory infiltration compared with WT mice, resulting in a significantly decreased cumulative histological score (Figure 1g). Certain cytokines and proinflammatory mediators contribute to the pathogenicity of human IBD and are reportedly increased in DSS-induced colitis.<sup>18</sup> We therefore investigated whether the attenuation in acute DSS-induced colitis, which was observed in  $\beta 7$ -integrin  $\Delta/\Delta$  mice, was reflected by changes in the expression levels of some of these mediators in colonic tissue homogenates or serum samples. Upon DSS treatment, all mice showed a significant enhancement in the colonic mRNA levels for tumor necrosis factor- $\alpha$  (TNF- $\alpha$ ), interleukin-6 (IL-6), interferon- $\gamma$  (IFN- $\gamma$ ), tumor growth factor- $\beta$  (TGF- $\beta$ ), C-C chemokine ligand-2 (CCL-2), and inducible nitric oxide reductase (iNOS). Interestingly,  $\beta 7$ -integrin  $\Delta/\Delta$  mice exhibited a reduced trend in the expression of the proinflammatory iNOS, CCL-2, IL-6, and TNF- $\alpha$  (Figure 2a), the latter was confirmed as significant when measured as protein level in serum (Figure 2b). By contrast, the expression of the anti-inflammatory cytokine TGF- $\beta$  appeared to be increased (Figure 2a).

#### Amelioration of DSS-induced colitis in $\beta 7$ -integrin $\Delta/\Delta$ mice is accompanied by a diminished influx of myeloid cells

Colonic histology from DSS-treated  $\beta 7$ -integrin  $\Delta/\Delta$  mice on hematoxylin and eosin sections (Figure 1d) revealed decreased inflammatory cell infiltrates compared with similarly treated WT controls. To analyze the inflammatory infiltrate in more detail, colon sections were stained for chloroacetate esterase (CAE), which identifies the lineage-specific cytoplasmic granules of myeloid cells (mast cells, neutrophils, and macrophages). Figure 3a shows CAE staining of colon sections from DSS-treated WT mice and  $\beta 7$ -integrin  $\Delta/\Delta$  mice. Interestingly, a marked increase in the number of red stained CAE<sup>+</sup> cells was noted in DSS-treated WT mice, which was less prominent in equally treated  $\beta 7$ -integrin  $\Delta/\Delta$  mice. Quantification of CAE<sup>+</sup> cells showed that loss of  $\beta 7$ -integrin significantly attenuates myeloid cell infiltration in response to DSS (Figure 3b). To characterize the effects of  $\beta 7$ -integrin on the immigration of myeloid cells more precisely, we performed

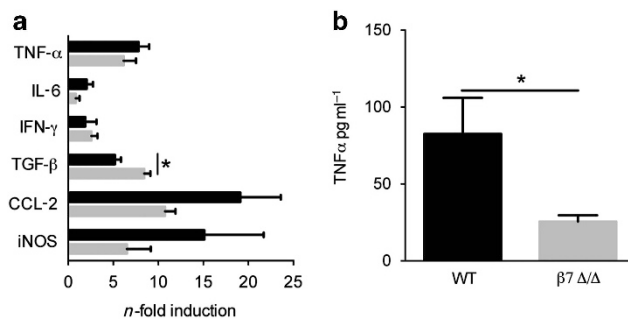


**Figure 2**  $\beta 7$ -Integrin deficiency results in decreased production of dextran sodium sulfate (DSS)-induced proinflammatory mediators. (a) Levels of the indicated mRNAs were measured in colon tissue at day 10 of acute DSS colitis. For quantification, values are expressed as fold increase over the mean values obtained for healthy control colon tissue. Black bars represent data from wild-type (WT) mice ( $n = 4$ ), gray bars from  $\beta 7$ -integrin-deficient ( $\beta 7\Delta/\Delta$ ) ( $n = 4$ ) mice, tumor necrosis factor- $\alpha$  (TNF- $\alpha$ ), interleukin-6 (IL-6), interferon- $\gamma$  (IFN- $\gamma$ ), tumor growth factor- $\beta$  (TGF- $\beta$ ), C-C chemokine ligand-2 (CCL-2), and inducible nitric oxide reductase (iNOS). Data represent mean  $\pm$  s.e.m. (b) TNF- $\alpha$  levels were measured in the serum from WT ( $n = 5$ ) and  $\beta 7\Delta/\Delta$  mice ( $n = 5$ ) at day 10 of acute DSS colitis. The data shown are representative of two independent experiments. Statistical significance was calculated by two-tailed  $t$ -test and is indicated as followings: \* $P < 0.05$ .

flow cytometric analysis on colonic cells of healthy and colitic WT and  $\beta 7$ -integrin  $\Delta/\Delta$  mice. DSS exposure (day 10 of acute DSS colitis) induced a marked influx of lymphocytes into the colon, which was reduced overall in  $\beta 7$ -integrin  $\Delta/\Delta$  mice and most noticeable for CD3<sup>+</sup> T cells (Supplementary Figure 1A–C online). This result was expected as  $\beta 7$ -integrin is known to regulate gut homing of lymphocytes. Without DSS treatment there was no obvious difference in the number and composition of myeloid cell populations between WT and  $\beta 7$ -integrin  $\Delta/\Delta$  mice. Interestingly, the fraction of the inflammatory infiltrate that consisted of CD11c<sup>+</sup>CD11b<sup>+</sup> cells from the innate immune system seemed to be reduced in DSS-treated  $\beta 7$ -integrin  $\Delta/\Delta$  mice when compared with WT mice (Supplementary Figure 1D). Further delineation of the CD11b<sup>+</sup> cell population revealed that although there was no significant difference in the number of immigrated CD45<sup>+</sup>Ly6G<sup>-</sup>CD11b<sup>+</sup>F4/80<sup>-</sup>GR1<sup>+</sup> cells (granulocytes; Supplementary Figure 1E), the fraction of CD45<sup>+</sup>Ly6G<sup>-</sup>CD11b<sup>+</sup>F4/80<sup>+</sup>GR1<sup>+</sup> cells, which have been described as inflammatory monocytes,<sup>19</sup> was reduced in DSS-treated  $\beta 7$ -integrin  $\Delta/\Delta$  mice when compared with equally treated WT mice (Figure 3c).

#### Aggravation of DSS-induced colitis by $\beta 7$ -integrin is mediated by cells of the innate immune system

Because it has been shown that lymphocytes may contribute to the outcome of DSS-induced colitis,<sup>20,21</sup> we compared the outcome of DSS-induced colitis in RAG-2  $\Delta/\Delta$  and RAG-2/ $\beta 7$ -integrin double-deficient mice, which lack mature T and B cells.<sup>22</sup>

As RAG-2  $\Delta/\Delta$  mice responded to DSS treatment with even more severe colitis compared with WT mice, we reduced the

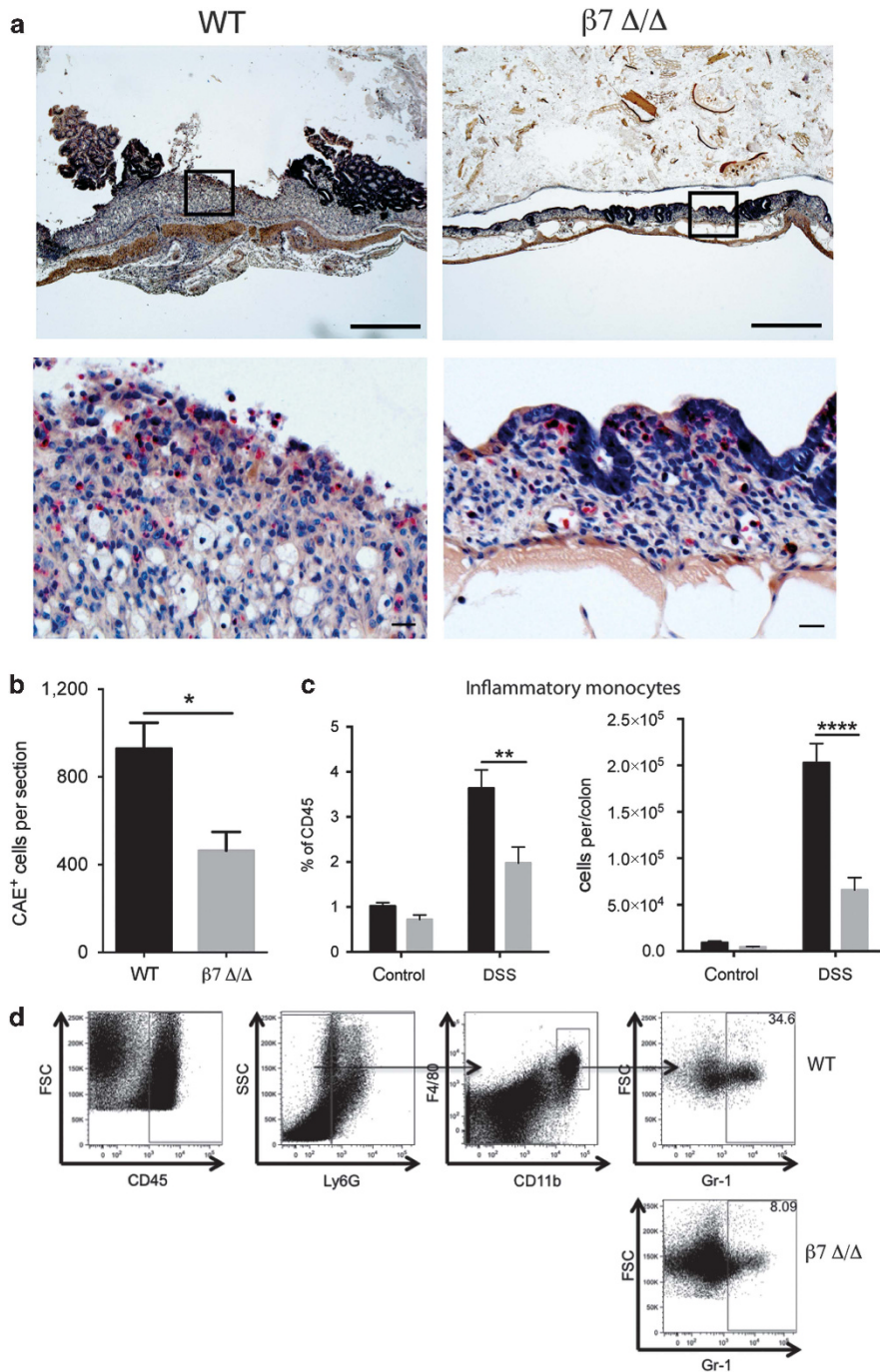


**Figure 3** Ameliorated colitis correlates with decreased immigration of myeloid cells in  $\beta 7$ -integrin-deficient mice. **(a)** Representative photomicrographs of chloroacetate esterase (CAE)-stained colon sections from the indicated groups (wild-type (WT),  $\beta 7$ -integrin-deficient ( $\beta 7\Delta/\Delta$ ) mice) at day 10 of acute dextran sodium sulfate (DSS) colitis at original magnification  $\times 5$  (Bar = 500  $\mu\text{m}$ ); boxed regions are shown below at original magnification  $\times 20$  (Bar = 20  $\mu\text{m}$ ). **(b)** Quantification of CAE<sup>+</sup> cells on sections from WT (black bar,  $n = 4$ ) and  $\beta 7 \Delta/\Delta$  (gray bar,  $n = 5$ ) mice. **(c)** Flow cytometric quantification of inflammatory monocytes (CD45<sup>+</sup> Ly6G<sup>-</sup> CD11b<sup>+</sup> F4/80<sup>+</sup> GR1<sup>+</sup>) in colon tissue of untreated and DSS-treated WT (black bar,  $n = 6$ ) and  $\beta 7 \Delta/\Delta$  (gray bar,  $n = 7$ ) mice at day 10 of acute DSS colitis shown as the percent of CD45<sup>+</sup> cells (left side) and as absolute number of cells per colon (right side). **(d)** Representative FACS dot plots illustrating the gating strategy for inflammatory monocytes of DSS-treated mice. The data shown are representative of two independent experiments. Statistical significance is indicated as follows: \* $P < 0.05$ , \*\* $P < 0.01$ , and \*\*\*\* $P < 0.0001$ . **(b)** Two-tailed  $t$ -test. **(c)** Two-way analysis of variance (ANOVA) with Sidak's post-test.

DSS dosage (2.5% DSS) to avoid mortality. Interestingly, when T and B cells were absent, the protective effect of the  $\beta 7$ -integrin deficiency was even more pronounced. As shown in **Figure 4**,

DSS administration to RAG-2  $\Delta/\Delta$  mice was associated with significant weight loss (**Figure 4a**) and clinical changes including diarrhea and occult fecal blood, resulting in a

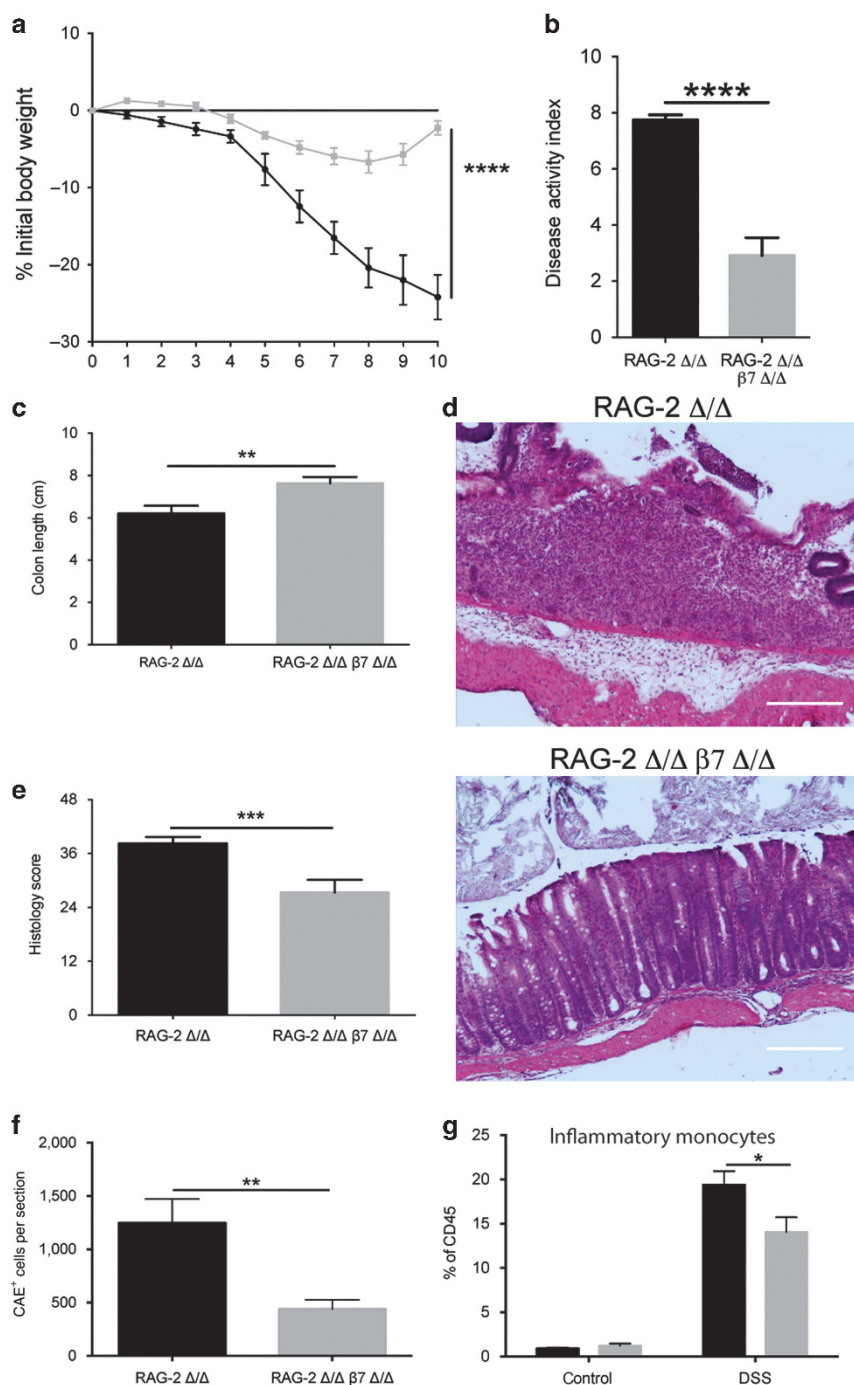


**Figure 4** Loss of  $\beta 7$  integrin protects recombination activating gene-2-deficient (RAG-2  $\Delta/\Delta$ ) mice from acute dextran sodium sulfate (DSS)-induced colitis. **(a)** Percentage of body weight loss (measured daily over the course of DSS treatment), **(b)** disease activity index (DAI), and **(c)** Colon length (at day 10 of acute DSS colitis) of RAG-2  $\Delta/\Delta$  (black squares, black bars,  $n = 12$ ) and RAG-2  $\Delta/\Delta$   $\beta 7$  integrin-deficient ( $\beta 7\Delta/\Delta$ ) (gray squares, gray bars,  $n = 13$ ) mice. **(d)** Representative photomicrographs of hematoxylin and eosin (H&E)-stained colon sections from the indicated groups at day 10 of acute DSS colitis at original magnification  $\times 100$  (bar represents  $100 \mu\text{m}$ ) and **(e)** results of histological scoring of sections from RAG-2  $\Delta/\Delta$  ( $n = 7$ ) and RAG-2  $\Delta/\Delta$   $\beta 7$  integrin  $\Delta/\Delta$  ( $n = 7$ ) mice. **(f)** Quantification of CAE<sup>+</sup> cells on sections from RAG-2  $\Delta/\Delta$  (black bar,  $n = 13$ ) and RAG-2  $\Delta/\Delta$   $\beta 7$  integrin  $\Delta/\Delta$  (gray bar,  $n = 11$ ) mice at day 10 of acute DSS colitis. **(g)** Flow cytometric quantification of inflammatory monocytes (CD45<sup>+</sup> Ly6G<sup>-</sup> CD11b<sup>+</sup> F4/80<sup>+</sup> GR1<sup>+</sup>) in colon tissue of untreated and DSS-treated RAG-2  $\Delta/\Delta$  (black bars,  $n = 5$  (untreated), 4 (DSS-treated)) and RAG-2  $\Delta/\Delta$   $\beta 7$  integrin  $\Delta/\Delta$  (gray bars,  $n = 3$  (untreated), 4 (DSS-treated)) mice at day 10 of acute DSS colitis. Gating was performed as illustrated in **Figure 3**. The data shown are representative of three independent experiments. Data represent mean  $\pm$  s.e.m. Statistical significance is indicated as follows: \* $P < 0.05$ ; \*\* $P < 0.01$ ; \*\*\* $P < 0.001$ ; \*\*\*\* $P < 0.0001$ . **(a–c, e, f)** Two-tailed  $t$ -test. **(g)** Two-way analysis of variance (ANOVA) with Sidak's post-test.

strongly increased cumulative DAI score (**Figure 4b**), whereas additional  $\beta 7$ -integrin deficiency resulted in a significant amelioration of DSS colitis. Consistently, DSS-treated RAG-2  $\Delta/\Delta$  mice showed a more severe reduction in colon length compared with DSS-treated RAG-2/ $\beta 7$  integrin double-deficient mice (**Figure 4c**). Moreover, DSS-treated RAG-2  $\Delta/\Delta$  mice exhibited more severe histopathology, accompanied by crypt destruction, mucosal ulcers, and erosions in the mucosal tissue, compared with the equally treated RAG-2/ $\beta 7$ -integrin double-deficient mice (**Figure 4d**), which was statistically confirmed by histological scoring (**Figure 4e**). Analysis for inflammatory markers revealed that exposure of RAG-2  $\Delta/\Delta$  mice to DSS resulted in enhanced colonic mRNA levels for IL-6, CCL-2, and iNOS, whereas in line with their immune-deficient status, we detected no induction of IFN- $\gamma$ . Compared with DSS-treated RAG-2  $\Delta/\Delta$  mice, equally treated RAG-2/ $\beta 7$ -integrin double-deficient mice exhibited an attenuation in the CCL-2 increase, measured as the protein level (RAG-2-deficient (RAG-2  $\Delta/\Delta$ ) + DSS:  $14.39 \pm 3.12$  pg mg $^{-1}$  colon tissue,  $n = 4$ ; RAG-2  $\Delta/\Delta$ ,  $\beta 7$   $\Delta/\Delta$ :  $6.17 \pm 0.9$  pg mg $^{-1}$  colon tissue,  $n = 6$ ;  $P = 0.0474$ ), and a reduced increase in colonic iNOS mRNA (RAG-2  $\Delta/\Delta$  + DSS:  $22.13 \pm 4.21$ -fold,  $n = 7$ ; RAG-2  $\Delta/\Delta$ ,  $\beta 7$   $\Delta/\Delta$ :  $8.17 \pm 1.614$ -fold increase,  $n = 5$ ;  $P = 0.0469$ ) (graphically displayed in **Supplementary Figure 2**).

Moreover, quantification of CAE $^{+}$  cells on colon sections of DSS-treated RAG-2/ $\beta 7$ -integrin double-deficient and RAG-2  $\Delta/\Delta$  mice showed that loss of  $\beta 7$ -integrin significantly attenuates myeloid cell infiltration in response to DSS (**Figure 4f**). Flow cytometric analysis of colonic cells of healthy and colitic animals revealed a decrease in the fraction of inflammatory monocytes (CD45 $^{+}$ Ly6G $^{-}$ CD11b $^{+}$ F4/80 $^{+}$ GRI $^{+}$  cells) in RAG-2/ $\beta 7$ -integrin double-deficient mice relative to RAG-2  $\Delta/\Delta$  mice (**Figure 4g**).

We also assessed the role of  $\beta 7$ -integrin on innate immune cells in the T-cell transfer model of chronic colitis.<sup>2</sup> This model is based on a disturbed T-cell homeostasis, which is caused by the adoptive transfer of CD4 $^{+}$ CD45RB $^{high}$  T cells (naïve T cells) from healthy WT mice into lymphopenic recipients and results in pancolitis and small bowel inflammation at 5–8 weeks following T-cell transfer. In the initial stage of this model, RAG-2/ $\beta 7$ -integrin double-deficient recipient mice exhibited an aggravated state of health (up to week 3; **Figure 5a, b**). However, there was no difference between the two mouse strains in the outcome of colitis 9 weeks after the cell transfer (**Figure 5a, c**), although we observed an increased number of inflammatory monocytes in the small intestine of colitic RAG-2  $\Delta/\Delta$  mice, which was attenuated in RAG-2/ $\beta 7$ -integrin double-deficient mice (**Figure 5d**).

### $\beta 7$ -Integrin contributes to colitis by promoting intestinal immigration of inflammatory monocytes

Intestinal macrophages are constantly replenished by Ly6C $^{+}$ CX3CR1 $^{int}$  blood monocytes that originate from the bone marrow.<sup>23,24</sup> Interestingly, 84% of the CD45 $^{+}$ CD11b $^{+}$ Ly6C $^{hi}$ CD64 $^{low}$  cells analyzed from the bone marrow of RAG-2

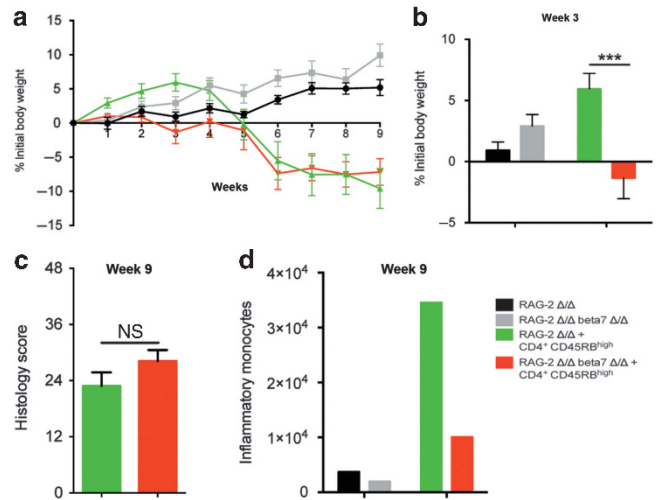


**Figure 5**  $\beta 7$ -Integrin on innate immune cells is of minor importance for the chronic stage of T-cell-mediated colitis. Recombination activating gene-2-deficient (RAG-2  $\Delta/\Delta$ ) and RAG-2  $\Delta/\Delta$   $\beta 7$ -integrin-deficient (RAG-2  $\Delta/\Delta$   $\beta 7\Delta/\Delta$ ) mice were adoptively transferred with  $0.5 \times 10^6$  CD4 $^{+}$ CD25 $^{-}$ CD45RB $^{hi}$  naïve T cells from wild-type mice and assessed for colitis development. Mice were weighed weekly. At 9 weeks after transfer, the mice were killed and analyzed by flow cytometry and histology. Color code: black = RAG-2  $\Delta/\Delta$  mice that received no cells (control); gray = RAG-2  $\Delta/\Delta$   $\beta 7\Delta/\Delta$  mice that received no cells (control); green = RAG-2  $\Delta/\Delta$  recipient mice that received CD4 $^{+}$ CD25 $^{-}$ CD45RB $^{hi}$  cells; red = RAG-2  $\Delta/\Delta$   $\beta 7\Delta/\Delta$  recipient mice that received CD4 $^{+}$ CD25 $^{-}$ CD45RB $^{hi}$  cells. **(a, b)** Body weight as a percent of starting weight of RAG-2  $\Delta/\Delta$  control mice (black,  $n = 5$ ), RAG-2  $\Delta/\Delta$   $\beta 7\Delta/\Delta$  control mice (gray,  $n = 5$ ), RAG-2  $\Delta/\Delta$  recipient mice (green,  $n = 11$ ), and RAG-2  $\Delta/\Delta$   $\beta 7\Delta/\Delta$  recipient mice (red,  $n = 11$ ) over the course of 9 weeks **(a)** and after 3 weeks **(b)**. **(c)** Results of histological scoring of sections from RAG-2  $\Delta/\Delta$  recipient mice (green,  $n = 8$ ) and RAG-2  $\Delta/\Delta$   $\beta 7$  integrin  $\Delta/\Delta$  recipient mice (red,  $n = 11$ ) mice after 9 weeks of chronic T-cell-mediated colitis. **(d)** Representative example of a flow cytometric quantification of inflammatory monocytes per small intestine (SI) after week 9 of chronic T-cell-mediated colitis of RAG-2  $\Delta/\Delta$  control mice (black), RAG-2  $\Delta/\Delta$   $\beta 7\Delta/\Delta$  control mice (gray), RAG-2  $\Delta/\Delta$  recipient mice (green), and RAG-2  $\Delta/\Delta$   $\beta 7\Delta/\Delta$  recipient mice (red). Flow cytometry data are from pooled small intestinal samples ( $n = 5$  mice each). The data shown are representative of two independent experiments. Data are presented as mean  $\pm$  s.e.m. Statistical significance was calculated by two-way analysis of variance (ANOVA) with Sidak's post-test and is indicated as follows: \*\*\* $P < 0.001$ .

$\Delta/\Delta$  mice coexpressed the gut homing receptor  $\beta 7$ -integrin (**Figure 6a**). To study the impact of  $\beta 7$ -integrin on the migration of monocytes from peripheral blood to the colon, we intravenously injected CD115-enriched 5-(and 6) carboxyfluorescein diacetate (CFSE)-labeled bone marrow cells (inflammatory monocytes) from  $\beta 7$ -integrin  $\Delta/\Delta$  or WT mice into DSS-treated RAG-2  $\Delta/\Delta$  mice. According to the literature,<sup>25</sup> these cells, which we characterized as CD45 $^{+}$ Ly6C $^{+}$ CD11b $^{+}$  cells, should represent mature inflammatory monocytes (**Supplementary Figure 3**). At 16 h after transfer, we monitored CFSE $^{+}$ CD11b $^{+}$ Ly6C $^{+}$  inflammatory monocytes that had arrived in different organs. There was no difference in the migration efficiency of CFSE $^{+}$   $\beta 7$ -integrin  $\Delta/\Delta$  or WT cells into the spleen, mesenteric lymph nodes, and peripheral lymph nodes (**Figure 6b** and data not shown). However, we detected a marked reduction in the number of

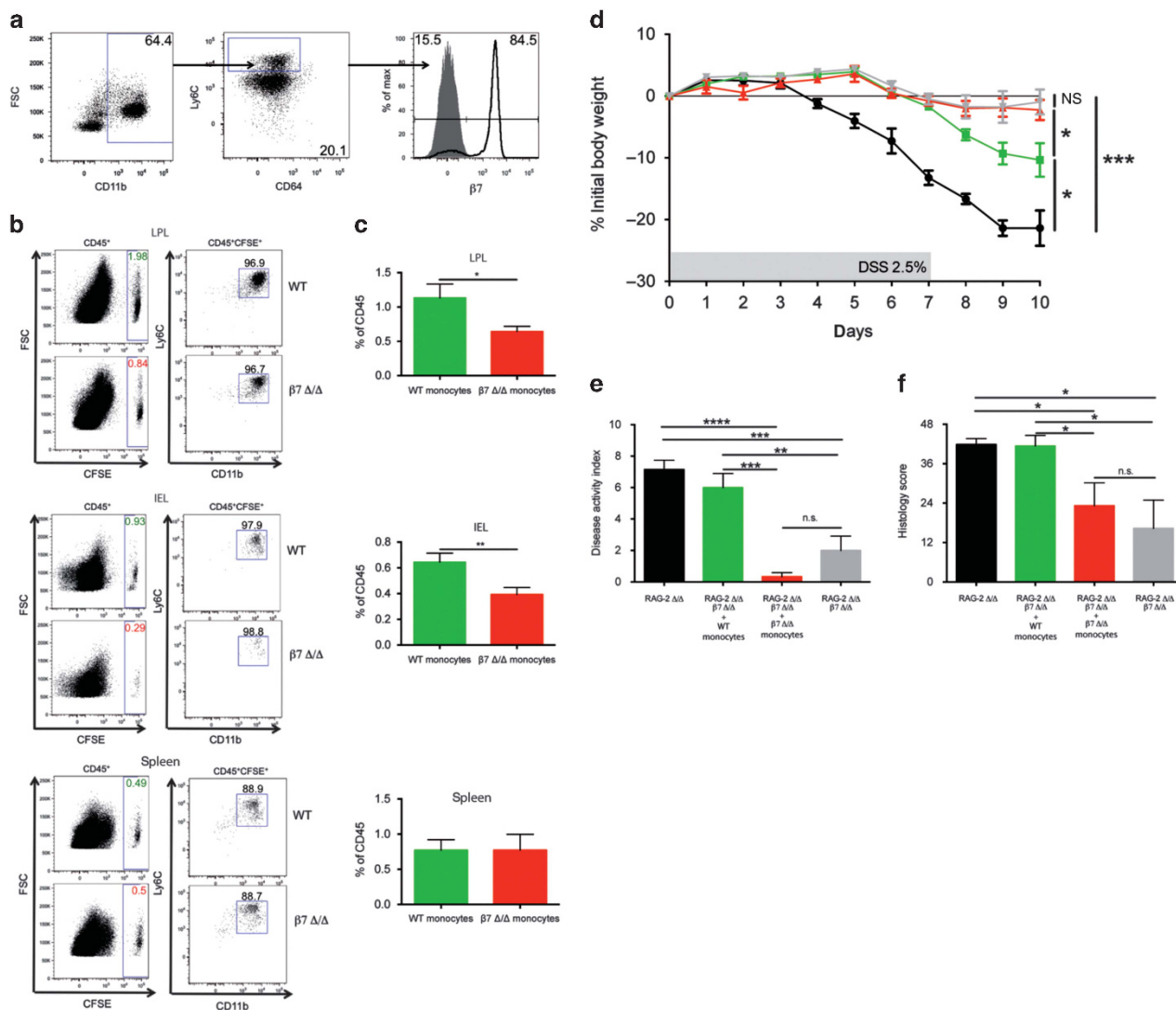


**Figure 6**  $\beta 7$ -Integrin-mediated immigration of inflammatory monocytes drives colitis. **(a)** Flow cytometric detection of  $\beta 7$ -integrin surface expression on  $CD45^{+}CD11b^{+}Ly6C^{hi}CD64^{low}$  cells isolated from bone marrow of recombination activating gene-2-deficient (RAG-2  $\Delta/\Delta$ ) mice. **(b and c)** Comparison of the migration efficiency of 5-(and 6) carboxyfluorescein diacetate (CFSE)-labeled  $CD115$ -enriched wild-type (WT) or  $\beta 7$ -integrin-deficient ( $\beta 7 \Delta/\Delta$ ) bone marrow monocytes into the colonic lamina propria lymphocyte (LPL) fraction, intraepithelial lymphocyte (IEL) fraction, and spleen of dextran sodium sulfate (DSS)-treated RAG-2  $\Delta/\Delta$  mice 16 h after intravenous transfer. **(b)** Representative FACS plots. **(c)** Quantification of immigrated  $CD45^{+}CFSE^{+}$  WT (green bars) and  $\beta 7 \Delta/\Delta$  (red bars) monocytes. Data are representative of three independent experiments. **(d)** Percentage (%) of body weight loss (measured daily over the course of DSS treatment), **(e)** disease activity index (DAI), and **(f)** histology score at day 10 of acute DSS colitis of RAG-2  $\Delta/\Delta$  mice (black squares, black bar,  $n = 7$ ), RAG-2  $\Delta/\Delta$ - $\beta 7 \Delta/\Delta$  mice (gray squares, gray bars,  $n = 4$ ), RAG-2  $\Delta/\Delta$ - $\beta 7$ -integrin  $\Delta/\Delta$  mice that had received WT monocytes (green squares, green bars,  $n = 5$ ), and RAG-2  $\Delta/\Delta$ - $\beta 7$ -integrin  $\Delta/\Delta$  mice that had received  $\beta 7 \Delta/\Delta$  monocytes (red squares, red bars,  $n = 5$ ). Data are representative of three independent experiments. Data represent mean  $\pm$  s.e.m. and significance is indicated as follows: NS = nonsignificant; \* $P < 0.05$ ; \*\* $P < 0.01$ ; \*\*\* $P < 0.001$ ; and \*\*\*\* $P < 0.0001$ . **(c)** One-tailed  $t$ -test. **(d-f)** One-way analysis of variance (ANOVA) with Tukey's post-test.

immigrated CFSE<sup>+</sup>  $\beta 7$ -integrin  $\Delta/\Delta$   $CD11b^{+}Ly6C^{+}$  cells in colonic intraepithelial lymphocyte and lamina propria lymphocyte fractions of colitic RAG-2  $\Delta/\Delta$  mice, when compared with the respective WT cells (**Figure 6b, c**).

Next, we assessed whether transfer of WT monocytes would aggravate the DSS-induced colitis in RAG-2/ $\beta 7$ -integrin double-deficient mice. To this end, we administered  $CD115$ -enriched bone marrow cells from WT mice intravenously into RAG-2/ $\beta 7$ -integrin double-deficient mice on the second day of DSS treatment (**Figure 6d-f**). The subsequent

development of colitis was assessed in comparison with that found in DSS-treated RAG-2/ $\beta 7$ -integrin double-deficient mice that had received an equal number of  $\beta 7$ -integrin  $\Delta/\Delta$   $CD115$ -enriched bone marrow cells and DSS-treated RAG-2/ $\beta 7$ -integrin double-deficient and DSS-treated RAG-2  $\Delta/\Delta$  mice without cell injection. Transfer of WT monocytes significantly increased DSS-induced colitis in RAG-2/ $\beta 7$ -integrin double-deficient mice, as evidenced by enhanced weight loss (**Figure 6d**) and cumulative DAI (**Figure 6e**), and more severe histopathology (**Figure 6f**), thereby restoring at least part

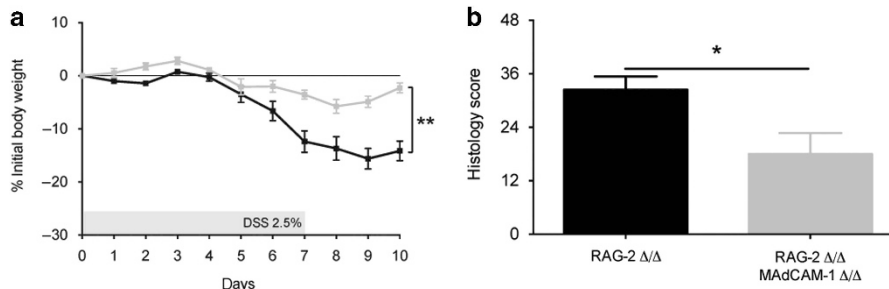


**Figure 7** MadCAM-1 (mucosal addressin cell-adhesion molecule-1)-deficiency ameliorates acute dextran sodium sulfate (DSS)-induced colitis. Disease severity is expressed in terms of (a) percentage (%) body weight loss (measured daily) and (b) results of histological scoring of sections from DSS-treated recombination activating gene-2-deficient (RAG-2  $\Delta/\Delta$ ) (black squares and bar,  $n=5$  (% initial body weight), 5 (histology score)), and RAG-2/MadCAM-1 double-deficient (RAG-2  $\Delta/\Delta$  MadCAM-1  $\Delta/\Delta$ ), (gray squares and bar,  $n=5$  (% initial body weight), 3 (histology score)) mice at day 10 of the experiment. The data are representative of three independent experiments and represent mean  $\pm$  s.e.m. Statistical significance was calculated by two-tailed *t*-test and is indicated as follows: \* $P<0.05$  and \*\* $P<0.01$ .

of the susceptibility to colitis seen in RAG-2  $\Delta/\Delta$  mice. DSS-treated RAG-2/ $\beta$ 7-integrin double-deficient mice that had received an equal number of  $\beta$ 7-integrin  $\Delta/\Delta$  CD115-enriched bone marrow cells also exhibited a trend towards aggravation of colitis, which was not however significant.

#### Amelioration of DSS colitis in RAG-2/MadCAM-1 double-deficient mice

$\beta$ 7-Integrin directs the migration of lymphocytes into the gut-associated lymphoid tissue mainly via its endothelial ligand MadCAM-1.<sup>4,26</sup> To find out whether MadCAM-1 also mediates the lymphocyte-independent role of  $\beta$ 7-integrin in DSS colitis, we studied the outcome of DSS colitis in RAG-2/MadCAM-1 double-deficient mice. Consistent with this hypothesis, body weight loss (Figure 7a) and cumulative DAI (not shown) were markedly attenuated in DSS-treated RAG-2/MadCAM-1 double-deficient mice relative to DSS-treated RAG-2 deficient mice. Histological examination and scoring of colon sections from DSS-treated RAG-2/MadCAM-1 double-deficient mice confirmed the reduced severity of inflammation when compared with DSS-treated RAG-2  $\Delta/\Delta$  mice (Figure 7b).

#### DISCUSSION

Preventing leukocyte recruitment to inflammatory sites by selectively interfering with leukocyte-endothelial interactions represents a promising strategy for IBD treatment. Recent clinical trials have shown that immunoneutralizing  $\alpha$ 4 $\beta$ 7-integrin with vedolizumab,  $\beta$ 7-integrin with etrolizumab, or MadCAM-1 with PF-00547659 significantly improves IBD.<sup>11</sup> However, the exact mechanism of action and the types of immune cells targeted by these anti-adhesion therapies have not yet been defined sufficiently. Up to now, the beneficial effects of a  $\beta$ 7-integrin blockage have been attributed to a blocking of the access of circulating T cells to the inflamed intestine.<sup>6,12,27–29</sup> However, in addition to its expression on lymphocytes,  $\alpha$ 4 $\beta$ 7-integrin is found on the surface of innate immune cells as well, and defects in innate immunity may be central to the pathogenesis of IBD.<sup>30</sup> Interestingly, we have

observed reduced numbers of conventional dendritic cells (DCs) and plasmacytoid DCs in the small intestinal IE compartment of MadCAM-1- $\Delta/\Delta$  and  $\beta$ 7-integrin  $\Delta/\Delta$  mice.<sup>31</sup> Moreover, two recent publications demonstrate that  $\alpha$ 4 $\beta$ 7-integrin directs the migration of a certain set of pre-mucosal DC progenitors from the bone marrow to the intestinal mucosa<sup>32</sup> and is required for the differentiation of intestinal CD11c<sup>+</sup> DCs with tolerogenic potential.<sup>33</sup> Herein, we show that  $\beta$ 7-integrin  $\Delta/\Delta$  mice exhibited attenuation in acute and chronic DSS-induced colitis. Amelioration of DSS colitis in  $\beta$ 7-integrin  $\Delta/\Delta$  mice was accompanied by a decreased influx of myeloid cells. The number of inflammatory monocytes in particular appeared to be reduced when compared with equally treated WT mice. Macrophage infiltration is a characteristic feature of IBD and is presumed to have a key role in IBD pathogenesis and DSS-induced colitis.<sup>34,35</sup> DSS has been shown to promote the recruitment of F4/80<sup>+</sup> CD11b<sup>+</sup> CCR2<sup>+</sup> Ly6C<sup>high</sup> inflammatory monocytes into the colon.<sup>36</sup> Moreover, microsphere-induced macrophage depletion,<sup>37</sup> neutralization of colony-stimulating factor-1, which is necessary for macrophage development,<sup>38</sup> or ablation of Ly6C<sup>high</sup> monocytes by anti-MC21 (CCR2) antibodies,<sup>39</sup> has been shown to alleviate DSS-induced colitis. Most of the TNF- $\alpha$ - or iNOS-producing cells in the inflamed colon of DSS-treated mice are reportedly monocytes or macrophages. The enzyme iNOS is essential for the generation of NO. It has also been detected in inflammatory infiltrates of the lamina propria and colonic epithelial cells in human IBD.<sup>40,41</sup> The pathogenic involvement of NO in DSS-induced colitis was evidenced by the fact that selective inhibitors of iNOS suppressed DSS-induced colonic inflammation.<sup>20,42</sup> Accordingly, we found a trend towards a reduced iNOS expression in the colon of DSS-treated  $\beta$ 7-integrin  $\Delta/\Delta$  mice when compared with equally treated WT mice. These results suggest that  $\beta$ 7-integrin deficiency ameliorates DSS-induced colitis by inhibition of the colonic immigration of proinflammatory monocytes and macrophages, thereby decreasing the production of proinflammatory mediators and inflammatory responses. DSS-induced colitis starts with disruption of the epithelium, followed by the activation of



macrophages and neutrophils, and does not depend on adaptive immunity.<sup>16</sup> However, T-cell responses in this model were shown to aggravate or ameliorate the inflammatory response in the presence of an intact innate and adaptive immunity and are especially involved in chronic DSS-induced colitis,<sup>43,44</sup> which was ameliorated by  $\beta 7$ -integrin deficiency. Whereas the T-cell response in the acute stage of DSS-induced colitis was described as a polarized Th1 response, the later and more chronic inflammation was characterized by a mixed Th1/Th2 response.<sup>44</sup> Furthermore, an involvement of CCR4-expressing effector T cells was reported in the development of DSS-induced colitis,<sup>45</sup> and adoptive transfer of primed T cells from DSS-treated mice was shown to aggravate DSS-induced colitis.<sup>46</sup> By contrast, lymphopenic mice were shown to be more susceptible to DSS-induced colitis,<sup>16,20</sup> indicating a protective role of lymphocytes in the inflammatory process, and deletion of FoxP3<sup>+</sup> regulatory T cell (Treg) in mice with an intact immune system caused an aggravation of DSS-induced colitis,<sup>47</sup> whereas CD25<sup>+</sup> Treg suppressed the inflammatory process in a TGF $\beta$ -dependent manner.<sup>48</sup> The ameliorated DSS-induced colitis in  $\beta 7$ -integrin  $\Delta/\Delta$  mice with an intact innate and adaptive immune system was accompanied by shifts in the number of colonic lymphocytes. To rule out their contribution to the inflammatory process, we analyzed the role of  $\beta 7$ -integrin in the pathogenesis of DSS colitis in lymphopenic RAG-2 mice. When compared with the respective WT mice, DSS-treated mice as well as untreated RAG-2 mice exhibited higher numbers of colonic inflammatory monocytes, which suggests a contribution of endogenous T cells to the control of colonic monocyte homeostasis and recruitment. In line with data from the literature,<sup>16,20</sup> RAG-2  $\Delta/\Delta$  mice were more susceptible to DSS colitis compared with WT mice, most probably because of the absence of protective Tregs.<sup>2,47,48</sup> Interestingly, colitis expression was much better tolerated in RAG-2/ $\beta 7$ -integrin double-deficient mice compared with that in RAG-2  $\Delta/\Delta$  mice, again accompanied by attenuated numbers of inflammatory monocytes and decreased expression of proinflammatory cytokines in the colon. Hence, the development of intestinal pathology in RAG-2  $\Delta/\Delta$  mice appears to be a  $\beta 7$ -integrin-mediated myeloid cell autonomous process, which does not depend on myeloid cell/lymphocyte interactions.

Of course, we cannot exclude that, in addition to inflammatory monocytes, other myeloid cell types contribute to the proinflammatory action of  $\beta 7$ -integrin in DSS-induced colitis. Although not significant, we observed a trend towards a reduction in the numbers of colonic granulocytes in  $\beta 7$ -integrin  $\Delta/\Delta$  mice, when compared with the respective WTs. These can include mast cells, basophils, neutrophils, and eosinophils. Depending on the experimental model of colitis used, all of these cell types have the potential to influence the degree of colitis in a pro- or anti-inflammatory manner. Basophils as well as mast cells express  $\beta 7$ -integrin. Recently, basophils were shown to exert beneficial effects in T-cell-mediated colitis,<sup>49</sup> whereas the involvement of mast cells in DSS-induced colitis, at least in immunocompetent mice, does not appear to be

crucial.<sup>50</sup> As neutrophils do not express  $\alpha 4\beta 7$ -integrin on their surface, differences in the immigration of neutrophils resulting from  $\beta 7$ -integrin deficiency would be secondary effects. Moreover, in the context of DSS-induced colitis, the role of colonic neutrophils seems to be beneficial in supporting antimicrobial defense and resolution of colitis.<sup>51</sup> Previously, we have shown, that  $\alpha 4\beta 7$ -integrin on eosinophils is crucial for eotaxin-1-mediated eosinophil recruitment into the small intestine,<sup>52</sup> whereas eosinophil accumulation in the colon in the context of DSS colitis can occur independently of  $\alpha 4\beta 7$ -integrin.<sup>53</sup> Although eosinophils have recently been described as promoters of chronic inflammation and tissue damage in chronic T-cell-dependent colitis,<sup>54</sup> they have been shown to exert protective effects in DSS-induced colitis.<sup>55</sup>

Intestinal macrophages develop from constantly arriving Ly6C<sup>+</sup>CX3CR1<sup>int</sup> blood monocytes.<sup>23</sup> In the healthy mouse mucosa, these monocytes are actively conditioned, as reported recently, upon sensing of IL-10,<sup>56</sup> to become nonmigratory and noninflammatory resident Ly6C<sup>+</sup>CX3CR1<sup>hi</sup> macrophages.<sup>39,57,58</sup> Acute inflammation, however, results in an increased immigration and impaired conditioning of these effector monocytes, thereby giving rise to CX3CR1<sup>int</sup> monocytes with proinflammatory, disease-promoting capacity.<sup>56,57</sup> Herein, we have shown that  $\beta 7$ -integrin is expressed on CD11b<sup>+</sup>CD64<sup>low</sup>Ly6C<sup>+</sup> monocytes, isolated from the bone marrow, and that  $\beta 7$ -integrin promotes the recruitment of these cells into the inflamed colon. Moreover, adoptive transfer of bone marrow-derived  $\beta 7$ -integrin-expressing monocytes into DSS-treated RAG-2/ $\beta 7$ -integrin double-deficient mice was sufficient to increase disease susceptibility. Therefore, it is most likely that the protective effects of a  $\beta 7$ -integrin deficiency on DSS colitis result from a disturbed colonic immigration of effector monocytes. Hence, the actions of  $\beta 7$ -integrin are more complex than originally assumed. As the intestinal homing molecule on lymphocytes, it contributes to immune defense,<sup>6</sup> T- and B-cell tolerance,<sup>59,60</sup> and T-cell-dependent colitis.<sup>6,12,28</sup> We have shown herein that  $\beta 7$ -integrin on inflammatory monocytes promotes colitis in the T-cell-independent DSS model. Therefore, the beneficial effects of a vedolizumab treatment in human IBD<sup>11</sup> are probably mediated not only by blocking the  $\beta 7$ -integrin-dependent access of circulating effector lymphocytes to the inflamed intestine but also by reducing the  $\beta 7$ -integrin-dependent influx of inflammatory monocytes. Moreover,  $\beta 7$ -integrin was shown to be involved in the intestinal recruitment of certain DC progenitors<sup>31,32</sup> and required for the anti-inflammatory actions of tolerogenic DC in experimental T-cell colitis.<sup>33</sup> The latter data from Villablanca *et al.*,<sup>33</sup> which show that mice lacking  $\beta 7$ -integrin in the innate immune compartment are more susceptible to T-cell-mediated colitis, are not in contrast to our findings. Also in our hands RAG-2/ $\beta 7$ -integrin double-deficient mice displayed an aggravated state of health in the initial stage of this model up to 3 weeks, when compared with the respective RAG-2 deficient mice. However, the animals recovered and we have noted no difference in disease severity between the two mouse strains in the later stages of disease (after 9 weeks), when T-cell-mediated

colitis is usually monitored.<sup>61</sup> Villablanca *et al.*<sup>33</sup> attribute their results to the reduced immigration of tolerogenic mononuclear phagocytes (ALDE<sup>+</sup>) in the mesenteric lymph nodes and small intestine of RAG2/ $\beta$ 7-integrin double-deficient mice, when compared with the respective RAG-2-deficient mice, in the early stage of disease. However, our results point to a minor function of these cells in the later stages of T-cell-mediated colitis. Although we have detected decreased numbers of inflammatory monocytes in the small intestine of RAG2/ $\beta$ 7-integrin  $\Delta/\Delta$  mice (in contrast to the respective RAG-2-deficient mice), there was no difference in the outcome of colitis. These findings hint at a minor function of tolerogenic and inflammatory monocytes in T-cell-mediated colitis.

Increased MAdCAM-1 expression on colonic vascular endothelial cells contributes to the infiltration of  $\alpha$ 4 $\beta$ 7-integrin-expressing effector T lymphocytes into inflamed gut lesions<sup>4</sup> and treatment with monoclonal MAdCAM-1-specific antibodies has been shown to ameliorate IBD in different animal models of colitis, a result that has so far been attributed to the blocked recruitment of lymphocytes.<sup>6,10</sup> Here, we have shown that genetic deletion of MAdCAM-1 in RAG-2  $\Delta/\Delta$  mice resulted in a similar protection against DSS-induced inflammation compared with RAG-2/ $\beta$ 7-integrin double-deficient mice. This finding suggests an additional function of MAdCAM-1 in promoting lymphocyte-independent colitis, by directing  $\beta$ 7-integrin-expressing innate immune cells to the inflamed intestine.

In conclusion, we have demonstrated that beyond its role in lymphocyte trafficking,  $\beta$ 7-integrin exacerbates colitis by promoting the accumulation of effector monocytes within the inflamed intestine, most probably mediated via interaction with MAdCAM-1. Thus, our study contributes to a better understanding of the cell migration pathways associated with the pathogenesis of experimental colitis and identifies inflammatory monocytes as a potential target for specific antiadhesive drugs.

## METHODS

**Mice.** All experiments were performed with male, age-matched mice of similar weight for the respective experimental groups, using 10- to 12-week-old  $\beta$ 7-integrin  $\Delta/\Delta$  mice (C57BL/6-Itgb<sup>tm1Cgm/J</sup>),<sup>3</sup> C57BL/6J mice (WT), RAG-2<sup>tm/J</sup> (RAG-2  $\Delta/\Delta$ ) mice,<sup>22</sup>  $\beta$ 7-integrin  $\Delta/\Delta$ -RAG-2  $\Delta/\Delta$  double-deficient mice, and MAdCAM-1-deficient (MAdCAM-1  $\Delta/\Delta$ ) mice (Madcam1<sup>tm1.2Nwag</sup>)<sup>26</sup>-RAG-2  $\Delta/\Delta$  double-deficient mice. Taking into consideration the three R's ("Replacement, Reduction, Refinement" of Russell and Burch, 1959), we reduced the number of animals used to a minimum. Whereas some material from acute DSS experiments was used to obtain additional information on the expression of inflammatory mediators, further material from the experiments was used for flow cytometric analysis (see below). The animals were bred in the same room at the RWTH Aachen under specific pathogen-free conditions and were free of *Helicobacter* spp. All experiments were approved by the Local Institutional Animal Care and Research Advisory Committee, and authorized by the local government authority (approval no. 84-02.04.2013.A153).

**Induction of colitis and determination of clinical scores.** Acute DSS colitis was induced by giving mice 2.5 or 3% (w v<sup>-1</sup>) DSS (molecular

mass, 36–50 kDa; MP Biomedicals, Solon, OH) in drinking water *ad libitum* for 7 days, which was replaced by normal drinking water for a recovery period until studies began at day 10. Chronic DSS colitis was induced by giving 3% (w v<sup>-1</sup>) DSS for 7 days, followed by 14 days of normal drinking water. This cycle was repeated two times until day 63.

To induce T-cell transfer colitis, splenocytes from WT mice were enriched for CD4<sup>+</sup> T cells by magnetic cell separation (MACS CD4<sup>+</sup> T-cell Isolation Kit; Miltenyi Biotec GmbH, Bergisch Gladbach, Germany). Cells were stained with anti-CD4-FITC (YTS 191.1.2) (ImmunoTools, Friesoythe, Germany), anti-CD45RB-PE (C 363.16 A) (eBioscience, San Diego, CA), and anti-CD25-APC (PC 61.5) (eBioscience) and sorted by flow cytometry (FACS Aria; BD Bioscience, Heidelberg, Germany). Phosphate-buffered saline (control) or  $0.5 \times 10^6$  CD4<sup>+</sup>CD25<sup>-</sup>CD45RB<sup>high</sup> cells in phosphate-buffered saline were injected intraperitoneally into RAG-2  $\Delta/\Delta$  or RAG-2/ $\beta$ 7-integrin double-deficient mice. Body weights and fecal status were followed and recorded weekly from the time of injection. Mice were killed at 9 weeks following adoptive transfer, by which time the recipients had lost ~10% of their initial body weight.

The DAI was assessed using a validated scoring system, as described previously by Osman *et al.*<sup>62</sup> Each animal was examined once a day and received a score on a scale of 0–4 for weight loss, stool consistency, and the presence of fecal blood. These features were averaged for each mouse and each group to calculate the DAI. The scores were defined as follows: weight loss—0 = body weight increased or remained within 1% of the baseline; 1 = 1–5% weight loss; 2 = 5–15% weight loss; 3 = 15–20% weight loss; and 4 = >20% weight loss. Stool consistency—0 = normal stools; 2 = loose stools; and 4 = diarrhea. The HemoCare test (Care Diagnostica, Voerde, Germany) was used to screen for occult blood in the stool and was scored as follows: 0 = negative test, no blood; 2 = positive test, moderate blood; and 4 = gross bleeding from the anus.

**Histological scoring.** The 4  $\mu$ m paraffin sections were serially cut, thereby dividing the Swiss-rolled colon into four levels of equal size, mounted onto glass slides, and deparaffinized. One section from each of the four levels was stained with hematoxylin and eosin by the Core Facility (IZKF) of the RWTH Aachen University. Blinded histological scoring was performed using a standard microscope, based on the method described previously.<sup>63</sup>

The naphthol-AS-D-chloroacetate esterase (CAE) staining was performed for each animal on one section from the middle of the colon, according to standard procedures. The number of positive red-stained leukocytes from 10 fields of vision (original magnification,  $\times 40$ ) was counted and averaged for each animal.

**Quantification of cytokines and chemokines.** Total RNA isolations from the distal part of the colon and cDNA synthesis were performed as described previously.<sup>63</sup> Real-time polymerase chain reaction was performed in duplicate in a total volume of 25  $\mu$ l, on a 7300 RT-PCR System with 7000 System SDS Software Version 1.2.3 (Applied Bioscience, Darmstadt, Germany) using the qPCR Master Mix for SYBR Green I (Eurogentec, Cologne, Germany) and specific primers for: glyceraldehyde-3-phosphate-dehydrogenase—sense, 5'-AGATGGTGATGGGCTTCCC-3'; antisense, 3'-GCCAAATTCAACGGCACAGT-5'; CCL-2—sense, 5'-GTGTTGGCTCAGCCAGATGC-3'; antisense, 3'-GACACCTGCTGCTGGTGATCC-5'; IFN- $\gamma$ —sense, 5'-GAGGTCAACAACCCACAGGTC-3'; antisense, 3'-CGAATCAGCAGCGACTCCT-5'; IL-6—sense, 5'-TGAGATCTACTCGGCAAACTAGTG-3'; antisense, 3'-CTTCGTAGAGAACAACATAAGTCA GATACC-5'; iNOS—sense, 5'-GGCAGCCTGTGAGACCCT-3'; antisense, 3'-TGAAGCGTTTCGGGATCTG-5'; TGF- $\beta$ —sense, 5'-GGACCCTGCCCTATATTTGG-3'; antisense, 3'-TGTTGCAGGTCATTTAACCAAGTG-5'; and TNF- $\alpha$ —sense, 5'-AGAAACACAA GATGCTGG GAC AGT-3'; antisense: 3'-CCT TTG CAG AAC TCA GGA ATG G-5'. Glyceraldehyde-3-phosphate dehydrogenase was used as an endogenous control for normalization. Expression levels of

the target genes are displayed as values relative to the level found in control animals (i.e. untreated C57BL/6 or RAG-2  $\Delta/\Delta$  mice).

Serum from cardiac blood was separated by centrifugation and kept at  $-80^{\circ}\text{C}$  until analysis. Fifty micrograms of colon tissue were homogenized in the lysis buffer (10 mM HEPES/2 mM EDTA/5 mM DTT/1 mM Pefablock; Sigma-Aldrich, Taufkirchen, Germany) containing Protease Inhibitor Cocktail (Roche, Mannheim, Germany). The homogenates were centrifuged at 4,000 g for 10 min, and the supernatants were stored at  $-80^{\circ}\text{C}$  for further analysis. Protein concentrations were quantified by a Bradford assay (BioRad, Hercules, CA). TNF- $\alpha$  and CCL-2 were determined with commercial DuoSet ELISA TNF $\alpha$  and MCP-1 Kits (R&D Systems, Minneapolis, MN) according to the manufacturer's instructions.

**Flow cytometry.** Cell isolation and surface staining were performed as described previously<sup>59</sup> using the following antibody conjugates: anti-CD8-PB (53–6.7), anti-CD11b-PB (M1/70), anti-CD11c-APC (N418), anti-CD11c-PE-Cy7 (N418), anti-CD115-bio (AFS98), anti-F4/80-APC (BM8), anti-Gr1-FITC (Ly6G/C, RB6-8C5), anti-Gr1-PE-Cy5 (Ly6G/C, RB6-8C5), anti-PDCA-1-APC (eBio128c1), Str.-PE-Cy7 (all from eBioscience), anti-CD3-FITC/145-2C11), anti-CD4-APC (RM4-5), anti-C19-APC (1D3), anti-CD45-APC-Cy7 (30-F11), Ly6C-PerCp-Cy5.5 (AL21), anti-Ly6G-FITC (1A8), anti-B7-PE (M293) (all from BD Bioscience), anti-mouse F4/80-RPE (C1:A3-1) (from Serotec, Oxford, UK), and anti-mouse CD64-Brilliant Violet 421 (X54-5/7.1) (BioLegend, Fell, Germany). Cells were measured on a FACS Canto II (BD Bioscience). Inflammatory monocytes were defined as CD45<sup>+</sup>Ly6G<sup>-</sup> (clone 1A8)CD11b<sup>+</sup>F4/80<sup>+</sup>GR1<sup>+</sup> cells in **Figures 3, 4** and **Figure 5**, and as a new monoclonal antibody was available, as CD45<sup>+</sup>Ly6C<sup>+</sup> (clone AL-21) CD11b<sup>+</sup> cells in **Figure 6**. Data were analyzed by the FlowJo 8.7.3 software (Tree Star, Ashland, OR).

**Isolation, CFSE labeling, and adoptive transfer of bone marrow monocytes.** CD115<sup>+</sup> bone marrow cells were purified by MACS using an anti-CD115 biotinylated antibody, followed by antibiotin microbeads (Miltenyi Biotec GmbH) according to the manufacturer's instructions. Purity of the enriched cell fraction was controlled by staining a sample of these cells with an antibody cocktail containing anti-CD45 and anti-Ly6C and was consistently 95% (shown as representative FACS plot in **Supplementary Figure 3**). The cells were resuspended in an appropriate volume of sterile phosphate-buffered saline allowing for  $2 \times 10^6$  cells per tail vein injection and were transferred once, on the second day of DSS treatment.

For CFSE labeling,  $5 \times 10^7$  cells were incubated in 5 ml RPMI + 25 mM HEPES for 30 min at  $37^{\circ}\text{C}$ . Thereafter, the cells were stained with  $1 \mu\text{M}$  CFSE for 10 min at  $37^{\circ}\text{C}$  in the dark. The labeling reaction was stopped by washing with phosphate-buffered saline/0.5% bovine serum albumin.

**Data analysis.** Statistical analyses were performed with GraphPad Prism software (version 5; GraphPad, La Jolla, CA).

Data are presented as mean  $\pm$  s.e.m., unless otherwise indicated. The specific statistical tests are indicated in the respective figure legends.

**SUPPLEMENTARY MATERIAL** is linked to the online version of the paper at <http://www.nature.com/mi>

#### ACKNOWLEDGMENTS

We thank B. Scholl for expert technical help. The research reported in this article was supported by a grant from the Deutsche Forschungsgemeinschaft (WA 1127/2-2).

#### DISCLOSURE

The authors declared no conflict of interest.

#### REFERENCES

- Springer, T.A. Traffic signals for lymphocyte recirculation and leukocyte emigration: The multistep paradigm. *Cell* **76**, 301–314 (1994).
- Powrie, F. T cells in inflammatory bowel disease: protective and pathogenic roles. *Immunity* **3**, 171–174 (1995).
- Wagner, N. *et al.* Critical role for beta7 integrins in formation of the gut-associated lymphoid tissue. *Nature* **382**, 366–370 (1996).
- Berlin, C. *et al.* Alpha 4 beta 7 integrin mediates lymphocyte binding to the mucosal vascular addressin MAdCAM-1. *Cell* **74**, 185–195 (1993).
- Briskin, M.J., McEvoy, L.M. & Butcher, E.C. MAdCAM-1 has homology to immunoglobulin and mucin-like adhesion receptors and to IgA1. *Nature* **363**, 461–464 (1993).
- Gorfu, G., Rivera-Nieves, J. & Ley, K. Role of beta7 integrins in intestinal lymphocyte homing and retention. *Curr. Mol. Med.* **9**, 836–850 (2009).
- Gallatin, W.M., Weissman, I.L. & Butcher, E.C. A cell-surface molecule involved in organ-specific homing of lymphocytes. *Nature* **304**, 30–34 (1983).
- van Zante, A. & Rosen, S.D. Sulphated endothelial ligands for L-selectin in lymphocyte homing and inflammation. *Biochem. Soc. Trans.* **31**, 313–317 (2003).
- Butcher, E.C., Williams, M., Youngman, K., Rott, L. & Briskin, M. Lymphocyte trafficking and regional immunity. *Adv. Immunol.* **72**, 209–253 (1999).
- Kato, S. *et al.* Amelioration of murine experimental colitis by inhibition of mucosal addressin cell adhesion molecule-1. *J. Pharmacol. Exp. Ther.* **295**, 183–189 (2000).
- Danese, S. & Panes, J. Development of drugs to target interactions between leukocytes and endothelial cells, and treatment algorithms for inflammatory bowel diseases. *Gastroenterology* **147**, 981–989 (2014).
- Sydora, B.C. *et al.* Beta7 integrin expression is not required for the localization of T cells to the intestine and colitis pathogenesis. *Clin. Exp. Immunol.* **129**, 35–42 (2002).
- Okayasu, I., Hatakeyama, S., Yamada, M., Ohkusa, T., Inagaki, Y. & Nakaya, R. A novel method in the induction of reliable experimental acute and chronic ulcerative colitis in mice. *Gastroenterology* **98**, 694–702 (1990).
- Kiesler, P., Fuss, I.J. & Strober, W. Experimental models of inflammatory bowel diseases. *Cell Mol. Gastroenterol. Hepatol.* **1**, 154–170 (2015).
- Melgar, S. *et al.* Validation of murine dextran sulfate sodium-induced colitis using four therapeutic agents for human inflammatory bowel disease. *Int. Immunopharmacol.* **8**, 836–844 (2008).
- Dieleman, L.A., Ridwan, B.U., Tennyson, G.S., Beagley, K.W., Bucy, R.P. & Elson, C.O. Dextran sulfate sodium-induced colitis occurs in severe combined immunodeficient mice. *Gastroenterology* **107**, 1643–1652 (1994).
- Axelsson, L.G., Landstrom, E., Goldschmidt, T.J., Gronberg, A. & Bylund-Fellenius, A.C. Dextran sulfate sodium (DSS) induced experimental colitis in immunodeficient mice: effects in CD4(+) cell depleted, athymic and NK-cell depleted SCID mice. *Inflamm. Res.* **45**, 181–191 (1996).
- Bento, A.F. *et al.* Evaluation of chemical mediators and cellular response during acute and chronic gut inflammatory response induced by dextran sodium sulfate in mice. *Biochem. Pharmacol.* **84**, 1459–1469 (2012).
- Dunay, I.R. *et al.* Gr1(+) inflammatory monocytes are required for mucosal resistance to the pathogen *Toxoplasma gondii*. *Immunity* **29**, 306–317 (2008).
- Kriegelstein, C.F. *et al.* Collagen-binding integrin alpha1beta1 regulates intestinal inflammation in experimental colitis. *J. Clin. Invest.* **110**, 1773–1782 (2002).
- Kim, T.W. *et al.* Involvement of lymphocytes in dextran sulfate sodium-induced experimental colitis. *World J. Gastroenterol.* **12**, 302–305 (2006).
- Shinkai, Y. *et al.* Rag-2-deficient mice lack mature lymphocytes owing to inability to initiate v(dj) rearrangement. *Cell* **68**, 855–867 (1992).
- Bain, C.C. *et al.* Constant replenishment from circulating monocytes maintains the macrophage pool in the intestine of adult mice. *Nat. Immunol.* **15**, 929–937 (2014).
- Varol, C. *et al.* Intestinal lamina propria dendritic cell subsets have different origin and functions. *Immunity* **31**, 502–512 (2009).
- De Kleer, I., Willems, F., Lambrecht, B. & Goriely, S. Ontogeny of myeloid cells. *Front. Immunol.* **5**, 423 (2014).

26. Schippers, A. *et al.* Mucosal addressin cell-adhesion molecule-1 controls plasma-cell migration and function in the small intestine of mice. *Gastroenterology* **137**, 924–933 (2009).
27. Kurmaeva, E., Boktor, M., Zhang, S., Bao, R., Berney, S. & Ostanin, D.V. Roles of T cell-associated I-selectin and beta7 integrins during induction and regulation of chronic colitis. *Inflamm. Bowel. Dis.* **19**, 2547–2559 (2013).
28. Picarella, D., Hurlbut, P., Rottman, J., Shi, X., Butcher, E. & Ringler, D.J. Monoclonal antibodies specific for beta 7 integrin and mucosal addressin cell adhesion molecule-1 (MAdCAM-1) reduce inflammation in the colon of SCID mice reconstituted with CD45RBhigh CD4+ T cells. *J. Immunol.* **158**, 2099–2106 (1997).
29. Apostolaki, M. *et al.* Role of beta7 integrin and the chemokine/chemokine receptor pair CCL25/CCR9 in modeled TNF-dependent Crohn's disease. *Gastroenterology* **134**, 2025–2035 (2008).
30. Farache, J., Zigmund, E., Shakhar, G. & Jung, S. Contributions of dendritic cells and macrophages to intestinal homeostasis and immune defense. *Immunol. Cell. Biol.* **91**, 232–239 (2013).
31. Clahsen, T., Pabst, O., Tenbrock, K., Schippers, A. & Wagner, N. Localisation of dendritic cells in the gut epithelium requires MAdCAM-1. *Clin. Immunol.* **156**, 74–84 (2014).
32. Zeng, R. *et al.* Retinoic acid regulates the development of a gut-homing precursor for intestinal dendritic cells. *Mucosal Immunol.* **6**, 847–856 (2013).
33. Villablanca, E.J. *et al.* Beta7 integrins are required to give rise to intestinal mononuclear phagocytes with tolerogenic potential. *Gut* **63**, 1431–1440 (2014).
34. Zigmund, E. & Jung, S. Intestinal macrophages: well educated exceptions from the rule. *Trends Immunol.* **34**, 162–168 (2013).
35. Kamada, N. *et al.* Unique CD14 intestinal macrophages contribute to the pathogenesis of crohn disease via IL-23/IFN-gamma axis. *J. Clin. Invest.* **118**, 2269–2280 (2008).
36. Waddell, A. *et al.* Colonic eosinophilic inflammation in experimental colitis is mediated by Ly6c(high) CCR2(+) inflammatory monocyte/macrophage-derived CCL11. *J. Immunol.* **186**, 5993–6003 (2011).
37. Nakase, H. *et al.* Development of an oral drug delivery system targeting immune-regulating cells in experimental inflammatory bowel disease: a new therapeutic strategy. *J. Pharmacol. Exp. Ther.* **292**, 15–21 (2000).
38. Marshall, D., Cameron, J., Lightwood, D. & Lawson, A.D. Blockade of colony stimulating factor-1 (CSF-1) leads to inhibition of DSS-induced colitis. *Inflamm. Bowel Dis.* **13**, 219–224 (2007).
39. Zigmund, E. *et al.* Ly6c hi monocytes in the inflamed colon give rise to proinflammatory effector cells and migratory antigen-presenting cells. *Immunity* **37**, 1076–1090 (2012).
40. Singer, I.I. *et al.* Expression of inducible nitric oxide synthase and nitrotyrosine in colonic epithelium in inflammatory bowel disease. *Gastroenterology* **111**, 871–885 (1996).
41. Godkin, A.J. *et al.* Expression of nitric oxide synthase in ulcerative colitis. *Eur J Clin Invest* **26**, 867–872 (1996).
42. Naito, Y. *et al.* The inducible nitric oxide synthase inhibitor ono-1714 blunts dextran sulfate sodium colitis in mice. *Eur. J. Pharmacol.* **412**, 91–99 (2001).
43. Jungbeck, M., Stopfer, P., Bataille, F., Nedospasov, S.A., Mannel, D.N. & Hehlgans, T. Blocking lymphotoxin beta receptor signalling exacerbates acute DSS-induced intestinal inflammation—opposite functions for surface lymphotoxin expressed by T and B lymphocytes. *Mol. Immunol.* **45**, 34–41 (2008).
44. Dieleman, L.A. *et al.* Chronic experimental colitis induced by dextran sulphate sodium (DSS) is characterized by Th1 and Th2 cytokines. *Clin. Exp. Immunol.* **114**, 385–391 (1998).
45. Mikami, S. *et al.* Blockade of CXCL12/CXCR4 axis ameliorates murine experimental colitis. *J. Pharmacol. Exp. Ther.* **327**, 383–392 (2008).
46. Shintani, N., Nakajima, T., Okamoto, T., Kondo, T., Nakamura, N. & Mayumi, T. Involvement of CD4+ T cells in the development of dextran sulfate sodium-induced experimental colitis and suppressive effect of IgG on their action. *Gen. Pharmacol.* **31**, 477–481 (1998).
47. Boehm, F. *et al.* Deletion of Foxp3+ regulatory T cells in genetically targeted mice supports development of intestinal inflammation. *BMC Gastroenterol.* **12**, 97 (2012).
48. Huber, S. *et al.* Cutting edge: TGF-beta signaling is required for the *in vivo* expansion and immunosuppressive capacity of regulatory CD4+ CD25+ T cells. *J. Immunol.* **173**, 6526–6531 (2004).
49. Gomez, M.R. *et al.* Basophils control T-cell responses and limit disease activity in experimental murine colitis. *Mucosal Immunol.* **7**, 188–199 (2014).
50. Minocha, A., Thomas, C. & Omar, R. Lack of crucial role of mast cells in pathogenesis of experimental colitis in mice. *Dig. Dis. Sci.* **40**, 1757–1762 (1995).
51. Zindl, C.L. *et al.* IL-22-producing neutrophils contribute to antimicrobial defense and restitution of colonic epithelial integrity during colitis. *Proc. Natl. Acad. Sci. USA* **110**, 12768–12773 (2013).
52. Mishra, A. *et al.* Enterocyte expression of the eotaxin and interleukin-5 transgenes induces compartmentalized dysregulation of eosinophil trafficking. *J. Biol. Chem.* **277**, 4406–4412 (2002).
53. Forbes, E. *et al.* ICAM-1-dependent pathways regulate colonic eosinophilic inflammation. *J. Leukocyte Biol.* **80**, 330–341 (2006).
54. Griseri, T. *et al.* Granulocyte macrophage colony-stimulating factor-activated eosinophils promote interleukin-23 driven chronic colitis. *Immunity* **43**, 187–199 (2015).
55. Masterson, J.C. *et al.* Eosinophil-mediated signalling attenuates inflammatory responses in experimental colitis. *Gut* **64**, 1236–1247 (2015).
56. Zigmund, E. *et al.* Macrophage-restricted interleukin-10 receptor deficiency, but not IL-10 deficiency, causes severe spontaneous colitis. *Immunity* **40**, 720–733 (2014).
57. Bain, C.C. *et al.* Resident and pro-inflammatory macrophages in the colon represent alternative context-dependent fates of the same Ly6chi monocyte precursors. *Mucosal Immunol.* **6**, 498–510 (2013).
58. Rivollier, A., He, J., Kole, A., Valatas, V. & Kelsall, B.L. Inflammation switches the differentiation program of Ly6Chi monocytes from anti-inflammatory macrophages to inflammatory dendritic cells in the colon. *J. Exp. Med.* **209**, 139–155 (2012).
59. Hadis, U. *et al.* Intestinal tolerance requires gut homing and expansion of Foxp3+ regulatory T cells in the lamina propria. *Immunity* **34**, 237–246 (2011).
60. Schippers, A. *et al.* Beta7 integrin controls immunogenic and tolerogenic mucosal B cell responses. *Clin. Immunol.* **144**, 87–97 (2012).
61. Ostanin, D.V. *et al.* T cell transfer model of chronic colitis: concepts, considerations, and tricks of the trade. *Am. J. Physiol. Gastrointest. Liver Physiol.* **296**, G135–G146 (2009).
62. Osman, N., Adawi, D., Ahrne, S., Jeppsson, B. & Molin, G. Modulation of the effect of dextran sulfate sodium-induced acute colitis by the administration of different probiotic strains of lactobacillus and bifidobacterium. *Dig. Dis. Sci.* **49**, 320–327 (2004).
63. Pils, M.C. *et al.* Commensal gut flora reduces susceptibility to experimentally induced colitis via t-cell-derived interleukin-10. *Inflamm. Bowel Dis.* **17**, 2038–2046 (2011).



This work is licensed under a Creative Commons Attribution-NonCommercial-NoDerivs 4.0 International License. The images or other third party material in this article are included in the article's Creative Commons license, unless indicated otherwise in the credit line; if the material is not included under the Creative Commons license, users will need to obtain permission from the license holder to reproduce the material. To view a copy of this license, visit <http://creativecommons.org/licenses/by-nc-nd/4.0/>